Journal of Applied Polymer Science

Morphological investigation of cellulose acetate/cellulose nanocrystal composites obtained by melt extrusion

Liliane Samara Ferreira Leite, Liliane Cristina Battirola, Laura Caetano Escobar da Silva, Maria do Carmo Gonçalves

Institute of Chemistry, University of Campinas (UNICAMP), P.O. Box 6154, Campinas, SP 13083-970, Brazil

Correspondence to: M. do Carmo Gonçalves (E-mail: maria@iqm.unicamp.br)

ABSTRACT: Composites were prepared from cellulose acetate (CA) and cellulose nanocrystals (CNC) by melt extrusion using two methods for the introduction of CNC: direct mixing and predispersion in CA solution. CNC were isolated using hydrochloric acid to increase thermal stability allowing the composites to be processed above 150 °C. The effect of CNC dispersion on the composites morphology, thermal, and mechanical properties was investigated. Field emission scanning electron microscopy and transmission electron microscopy results indicated that the predispersion method allows better CNC dispersion and distribution when compared to the direct mixture method. In addition, predispersion promotes preferential CNC orientation in relation to the injection flow. The predispersion method also showed a 14% Young's modulus increase in composites containing 15 wt % CNC while no significant change was observed when using the direct mixing. The results obtained in this work show that, to achieve the percolation threshold, nanoparticle distribution is as important as their content. © 2016 Wiley Periodicals, Inc. J. Appl. Polym. Sci. **2016**, *133*, 44201.

KEYWORDS: cellulose and other wood products; composites; extrusion; polysaccharides

Received 16 March 2016; accepted 10 July 2016

DOI: 10.1002/app.44201

INTRODUCTION

Cellulose nanocrystals (CNC) are highly attractive reinforcing agents in polymeric composites due to their low density, high elastic modulus, and stiffness as well as renewability and biodegradability. There are two routes that have been used to isolate CNC from natural fibers, either by mechanical treatments or by hydrolysis (enzymatic or acid).[1–3]

The most widely used acid in cellulose hydrolysis is sulfuric acid.[4–6] However, CNC obtained by sulfuric acid hydrolysis has poor thermal stability due to the remaining sulfate groups attached to their surface. This is a major drawback for CNC-based composites prepared by a broad range of processing methods, which are commonly used in the field of polymer science. To overcome this issue, some authors have used hydrochloric and phosphoric acids as attack-molecules for CNC isolation.[7,8] The use of these acids results in more thermally stable CNC. Typically, nanoparticles with needle-like morphology are obtained irrespective of the isolation process selected. Nevertheless, the cellulose source and isolation conditions determine the CNC dimensions, ranging from 5 to 30 nm in diameter and from 100 nm to several micrometers in length.[9,10]

Many studies have attempted to develop CNC-polymer composites using different polymer matrices, such as poly(lactic acid),[11,12] poly(ε-caprolactone),[13,14] polypropylene,[15] and polyethylene.[16] Among the cellulosic matrixes, cellulose acetate (CA) and CA butyrate[17,18] are the most studied. CA has the advantages of transparency, stiffness, water vapor permeation, as well as thermal and impact resistance.[19,20] The application of CA can be seen in several areas, such as filters,[21] membranes,[22,23] packing films,[24] coatings for paper,[25] and drug delivery[26–28] systems. The use of CNC could enhance the following characteristics in CA, such as poor dimensional stability and fair mechanical properties. However, the results shown in literature on bio-based materials that combine CA and CNC do not provide enough insights about structure-properties relationship of this bio-based composite.

In general, composite are produced by dispersing dried cellulose nanoparticles, fibers, or nanocrystals into a cellulose or cellulose derivative solution, followed by casting and drying.[17,29,30] This procedure, named solvent-casting, has some particular advantages such as good nanoparticle dispersion and readily available experimental equipment. However, in the thermoplastic processing industry, melt-extrusion associated with injection molding

Additional Supporting Information may be found in the online version of this article.

is the most important processing technique as it allows high production rate and the absence of a solvent. In addition, melt extrusion is suitable to high molecular weight polymers which is the case of cellulose derivatives.[31–33]

In spite of these advantages, little is the research that explores composite preparation by melt extrusion, probably due to the small gap between processing and degradation temperatures of cellulosic polymers. In addition, the CNC dispersion and distribution are also drawbacks that must be overcome in the composite field. To reach good CNC dispersion and distribution into the polymeric matrices, works in literature have shown the use of CNC predispersion. CNC predispersion can prevent premature CNC degradation and also contribute to increase homogeneity in CNC distribution. In this case, the Brownian motion can allow particle-particle interactions to take place.[34] A tentative of CNC predispersion in polymeric matrix was first published by Bondeson and Oksman.[35] In their work, CNC was predispersed in a poly(vinyl alcohol) solution, freeze dried and subsequently added to poly(lactic acid) prior to extrusion. Corrêa *et al.*[36] studied the predispersion of CNC in polyamide 6 solution prior to melt extrusion. The authors achieved a 45% increase in elastic modulus for composites containing 1 wt % CNC, which they attributed to the improvement in CNC dispersion. Well dispersed composites using CA butyrate as matrix was also achieved by CNC predispersion in a CA butyrate solution.[18] The effect of the CNC incorporation method on the composite mechanical properties is also described by Pracella *et al.*[37] who showed that the preparation of PLA nanocomposites, containing poly(vinyl acetate) dispersed CNC, increases the mechanical properties of these nanocomposites. The above examples indicate that the predispersion strategy is a useful and straightforward alternative to reach the appropriate CNC dispersion and, therefore, mechanical properties improvement. However, little work has been done in the sense of investigating CNC morphology, dispersion and distribution within a polymer matrix.

The importance to characterize the morphology of CNC-based composites is evident. The lack of studies that focus on the direct observation of the CNC distribution as well as dispersion onto polymer matrices by microscopy techniques is due to the fact that CNC composites do not provide enough contrast to clearly distinguish each phase.

Herein, composites combining CNC and CA prepared by melt extrusion are presented and their morphology investigated by field emission scanning electron microscope (FESEM) and transmission electron microscope (TEM). To achieve adequate thermal stability for processing with CA, CNC were isolated from cotton fibers by hydrochloric acid hydrolysis. The combination of solvent casting and melt extrusion methods was used in this work and compared to the direct mixing to verify the influence of the preparation method on the CNC dispersion and distribution in the CA matrix. This work focuses on the material morphology; however, thermal and mechanical properties of the composites were also investigated.

EXPERIMENTAL

Materials

Cotton fibers (York S/A), hydrochloric acid (37% purity, Synth), and triethyl citrate (TEC, Across Organics) plasticizer were used as received. CA (Eastman Chemicals) free of additives with a 50,000 g/mol number-average molecular weight and 38.7 wt % acetyl groups was dried under vacuum at 100 °C for 24 h prior to use.

Preparation of CNC

CNC were prepared using optimized conditions described in previous work.[38,39] Briefly, cotton fibers (1 g) were added to a hydrochloric acid solution (35 mL, 4 mol/L) at 80 °C and kept under stirring for 225 min, after which cold deionized water was added to stop hydrolysis. The excess acid was removed by repeated centrifugation cycles at 4000 rpm for 15 min. The resulting suspension was then dialyzed against running water until reaching a pH of 7. Lastly, the dialyzed aqueous suspension was lyophilized in a K105 Liotop equipment to obtain powdered CNC.

Predispersion of CNC in CA Matrix

Prior to melt extrusion, samples were prepared by the following method. First, CA was dissolved into acetone under magnetic stirring at 60 °C. After complete CA dissolution, TEC plasticizer was added to CA solution to obtain 70/30 CA/TEC weight ratio. This plasticizer content was chosen based on previous work[40] which aimed to optimize the plasticizer content for CA melt extrusion. Afterwards, fresh CNC aqueous suspension (12 wt %), obtained directly from dialysis, was added dropwise into the CA/TEC solution (24 wt %) and stirred for approximately 24 h. The water content in the final solution was controlled to maintain CA solubility. The obtained CA/TEC/CNC suspension was cast in Petri dishes and dried at room temperature until no evidence of residual solvent was detected. Finally, the casting films were milled in a Corning laboratory blender and dried at 60 °C for 48 h to obtain a CA/TEC/CNC powder.

Preparation of Composite via Melt Extrusion

The CA/TEC/CNC powder obtained previously was added to a predefined amount of CA/TEC 24 h prior to melt extrusion. Afterwards, this mixture was melt extruded by means of a 15 mL twin-screw CC15 microcompounder – DSM Xplore™. The melt extrusion processing occurred at 190 °C and 150 rpm for 3 min. The resulting composites were denoted as PD-CA/TEC/CNC5, PD-CA/TEC/CNC10, and PD-CA/TEC/CNC15. The numbers (5, 10, and 15) represent CNC content in weight percentage, and the letters "PD" indicate that CNC was predispersed in CA/TEC solution prior to melt extrusion. Composites with the same compositions were also prepared by direct mixture and were named D-CA/TEC/CNC5, D-CA/TEC/CNC10, and D-CA/TEC/CNC15, respectively. In this case, freeze-dried CNC was added directly to CA and TEC (70/30 wt %) and mixed 24 h prior to melt extrusion (conventional processing route). In the sequence, the extrudates were injection-molded in a 12 mL microinjector – DSM Xplore™ at 180 °C, mold temperature at 35 °C, and pressure of 6 bar for 10 s to obtain tensile test specimens according to ASTM D638-10. Same procedure was applied to prepare the reference CA/TEC 70/30 wt %.

Characterization

X-ray diffraction (XRD) measurements were carried out in an X-ray diffractometer (SHIMADZU XRD7000). XRD patterns were acquired using CuKα radiation ($k = 0.15406$ nm) at 40 kV,

30 mA and recorded in a 5° to 50° 2θ range. CNC degree of crystallinity (DC) was measured applying the Segal method,[41] and was calculated as follows:

$$DC=(I_{002}-I_{am})/I_{002}\times 100 \quad (1)$$

where, I_{002} is the maximum intensity of the 002 lattice diffraction (2θ ~ 22°) and I_{am} is the intensity of diffraction at 2θ ~ 18°.

Thermogravimetric analyses (TGA) were obtained in a 2950 TA instrument, in a 25 to 600 °C temperature range, at a 10 °C/min heating rate under Argon atmosphere. Approximately 10 mg samples were used.

Mechanical properties at tensile stress were obtained according to ASTM D638-10 in an EMIC DL 200 with a 5000 N load cell and 5 mm/min crosshead speed. The results were averaged over six measurements.

Dynamic mechanical analysis was carried out using a DMTA V Rheometric Scientific Instrument in a −150 to 150 °C temperature range at 2 °C/min. Rectangular samples (30 mm × 8.0 mm × 0.7 mm) were submitted to tension/compression deformation at a 1.0 Hz frequency and 0.02% amplitude.

CNC morphology was examined in a Carl Zeiss Libra 120 TEM equipped with an in-column OMEGA filter, at an acceleration voltage of 120 kV. Drops of diluted CNC/isopropanol suspensions were deposited on carbon coated parlodion films supported on copper grids and allowed to dry. Samples were stained with 2 wt % uranyl acetate solution for 2 min before analysis. CNC dimensions were measured using the ImageJ software. Composites were characterized using approximately 65 nm thick ultrathin sections, which were cut at −100 °C using a diamond knife in a Leica EM FC6 cryo-ultramicrotome. These sections were stained using a 2 wt % uranyl acetate solution to reveal the CNC. Images were recorded using an Olympus CCD camera 14 bits with 1736 × 1032 resolution.

The morphology of the cryogenically fractured samples was examined in a JEOL JSM-6340F FESEM, operating at an accelerating voltage of 3 kV. The CNC morphologies were also examined by dropping a water dispersion of CNC on a mica surface mounted in the sample holder. All samples were carbon and platinum sputter coated in a Bal-Tec MD 020 instrument from Balzers.

RESULTS AND DISCUSSION

Characterization of the CNC

Cotton fiber is a suitable CNC source due to its high cellulosic content (~90 wt %), in contrast with its low hemicellulose (~3–4 wt %) and lignin (in non-appreciable quantities) contents.[41] The crystalline structures of cotton fibers and CNC were determined by XRD and the results are shown in Figure 1 (a and b curves, respectively). Both samples presented typical diffraction peaks at 15°, 18°, 23°, and 34° (2θ), which are assigned to the Cellulose I (native cellulose) crystal unit.[42] The calculated degrees of crystallinity are 78% and 91%, for cotton fiber and CNC, respectively. The increase in crystallinity observed for CNC indicates the removal of cellulose amorphous content as well as other amorphous components through acid hydrolysis.

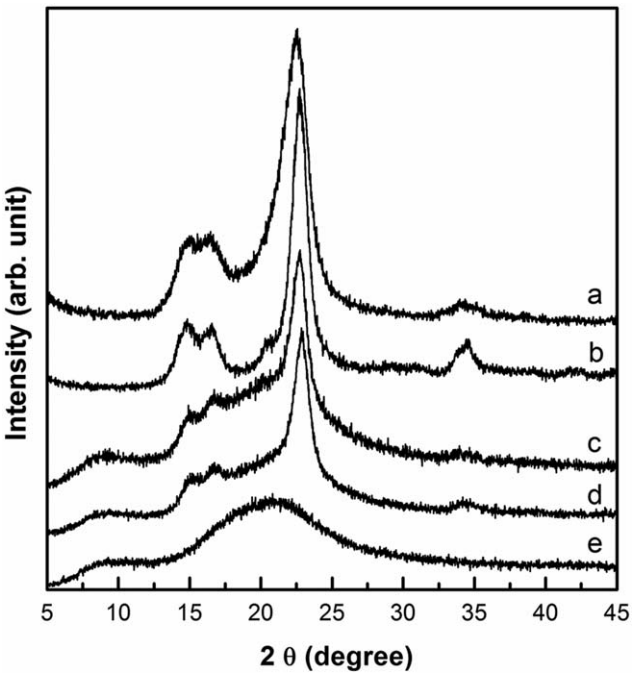

Figure 1. XRD patterns of (a) cotton fibers, (b) CNC, (c) PD-CA/TEC/CNC15, (d) D-CA/TEC/CNC15, and (e) CA/TEC matrix.

The CNC morphology was observed by FESEM and TEM. Representative images are shown in Figure 2(a,b). As observed, the acid attack was effective in obtaining nanoparticles with needle-like morphology through the cleavage of the interfibrilar links of the cotton fiber amorphous phase. However, the presence of some partially hydrolyzed fibers (arrows) at the FESEM micrograph [Figure 2(a)], is an indicative of the lower yields attained by hydrochloric acid hydrolysis. The circle shown in Figure 2(a) highlights the CNC aggregates.

It is widely known that the CNC average length is mainly dependent on the cellulosic source and on the hydrolysis conditions.[43] In this work, the average length (L) and diameter (d), determined by TEM, were found to be 231 ± 28 nm and 14 ± 3 nm, respectively, giving an average aspect ratio (L/d) of around 16. These values are in agreement with the ones previously reported[44,45] and were used to calculate the mechanical percolation threshold of the composites.

Characterization of Cellulose Composites

In this section, composite characterization will be shown and compared to the plasticized CA matrix (CA/TEC). For simplicity, only higher CNC content composites will be shown in the majority of the analyses. In this work, CNC predispersion in a CA/TEC solution was used to verify if in fact occurs the CNC distribution improvement in the CA matrix, as described in literature.[46,47]

Figure 1(c–e) shows the XRD patterns obtained for neat CA/TEC matrix and the CA/TEC/CNC composites containing 15 wt % CNC prepared by both methods. As an amorphous material, CA/TEC presents an amorphous halo around 22° and no crystalline peaks can be observed. Due to the high CNC content (15 wt %), diffraction peaks at 2θ of 15°, 18°, 23°, and 34° are also

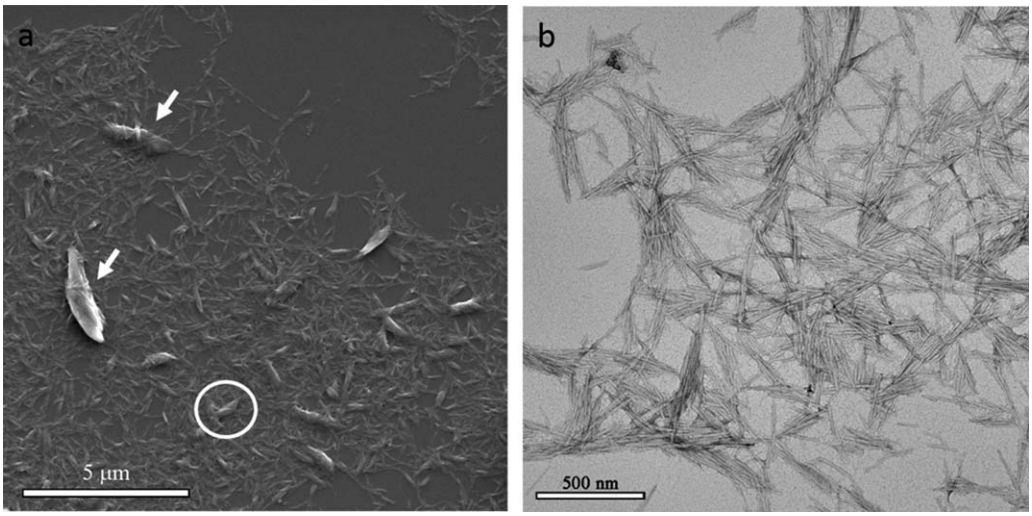

Figure 2. (a) FESEM and (b) TEM micrographs of cotton nanocrystals. Arrows show partially hydrolyzed fibers and circle highlight CNC aggregates.

shown for the composites, irrespective of the preparation method. These are typical diffraction peaks for Cellulose I, as already shown in Figure 1(a,b), and their presence in the composites confirms the integrity of CNC crystal structure after melt extrusion.

Figure 3 shows the thermal degradation behavior of CNC, CA/TEC matrix, and CA/TEC/CNC composites, which were investigated by thermogravimetric analysis. Generally, CNC presents distinct thermal degradation events depending on the acid used in the hydrolysis process. In the case of CNC isolated by hydrochloric acid, which was used in this work, the absence of charged groups on the CNC surface results in the onset thermal degradation temperature at 330 °C, which is approximately 180 °C higher than the commonly reported onset thermal degradation temperature for CNC isolated by sulfuric acid.[7] This degradation temperature is appropriate for nanocrystal processing with common polymer matrices. The thermal stability is one of the main issues in the processing of CNC reinforced polymer composites. In contrast, the CA/TEC matrix presents three regions of thermal degradation. The first one, ascribed to residual water volatilization, is in the range of 130 to 240 °C. The second one, ranging from 250 to 330 °C, is related to CA loss of acetyl groups in the form of acetic acid volatilization. For CA/TEC and composite samples, these two events can also correspond to the loss of TEC plasticizer. The last weight loss region, from 350 to 425 °C, is referred to as the thermal degradation of the cellulose main chain.[48–50] These results show that irrespective of the CNC addition method, no pronounced changes in the thermal degradation behavior are observed for the composites prepared. As discussed by Mariano *et al.*,[51] cellulose materials produce flammable volatile components at temperatures above 200 °C. The production of degradation gases promotes free space increase within the polymer matrix, which causes changes in the heat diffusion mechanism inducing polymer degradation. In the thermal analysis conditions used in this work, the absence of a new degradation event for the composites, at temperatures lower than 330 °C, as shown in Figure 3, is a valuable result for the CA/TEC/CNC composite melt extrusion process. This is due to the use of CNC obtained from hydrochloric acid hydrolysis. In this aspect, it is important to point out that the most common CNC used for composite preparation, which is obtained by sulfuric acid hydrolysis, not only presents lower thermal stability but can also induce polymer thermal degradation due to the presence of sulfate groups on the CNC surface.[7,52,53]

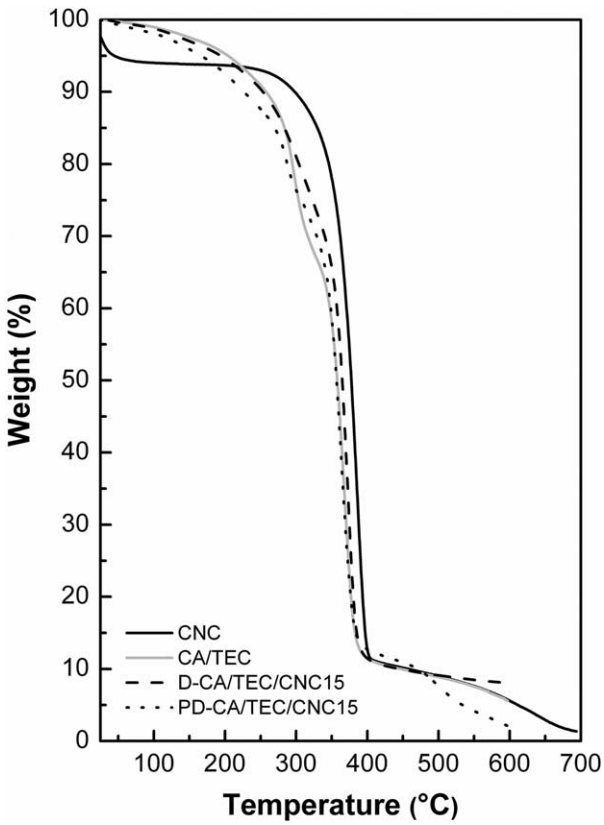

Figure 3. TGA curves of CNC, CA/TEC, D-CA/TEC/CNC15, and PD-CA/TEC/CNC15 composites.

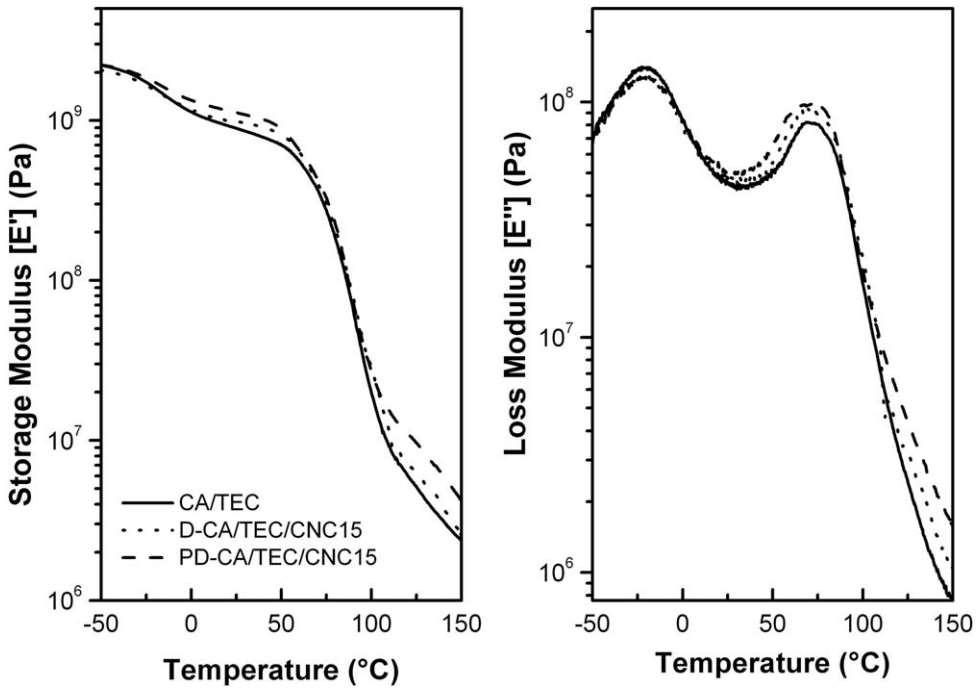

Figure 4. Storage (left) and loss (right) moduli of CA/TEC, D-CA/TEC/CNC15, and PD-CA/TEC/CNC15 composites.

To further investigate the effect of CNC addition on the composite mechanical properties, D-CA/TEC/CNC15 and PD-CA/TEC/CNC15 samples were also analyzed in terms of dynamic mechanical behavior and compared to the CA/TEC matrix (Figure 4). This analysis provides qualitative information on the polymer relaxation spectra as well as some important thermal

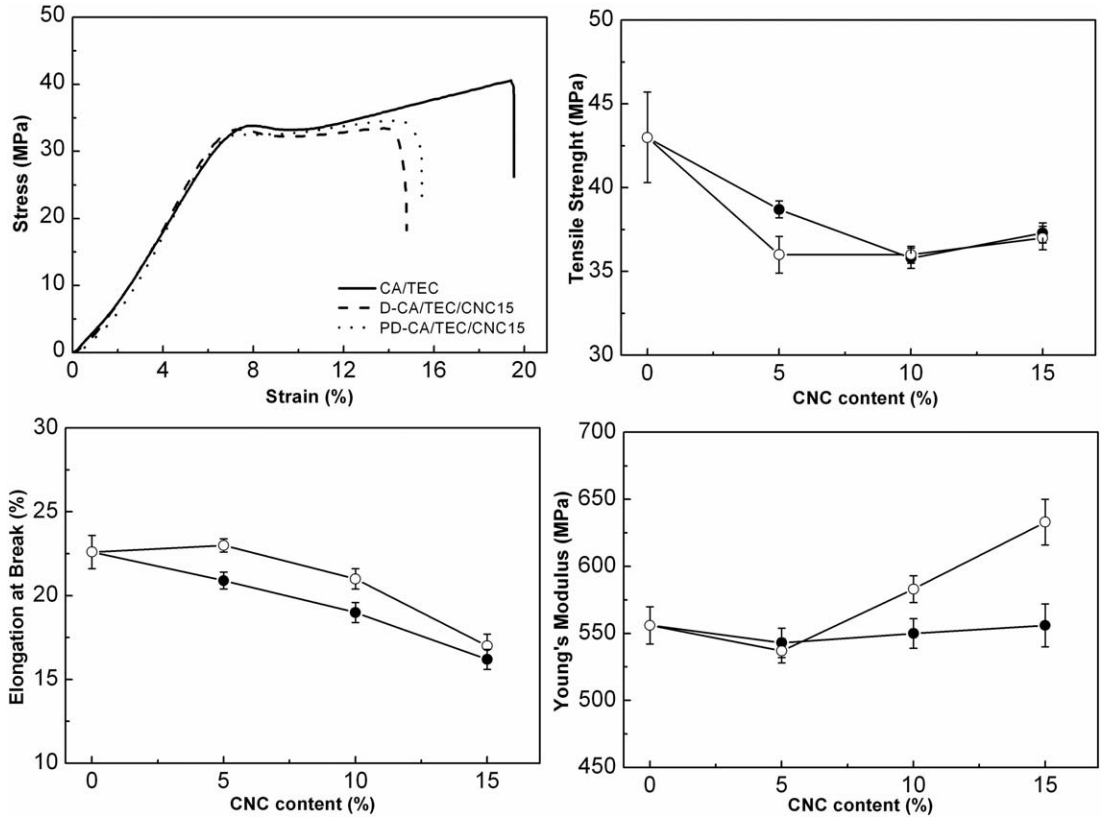

Figure 5. (a) Stress–strain curves, (b) tensile strength, (c) elongation at break, and (d) Young's modulus, as a function of CNC content in CA/TEC, D-CA/TEC/CNC15 (●), and PD-CA/TEC/CNC15 (○).

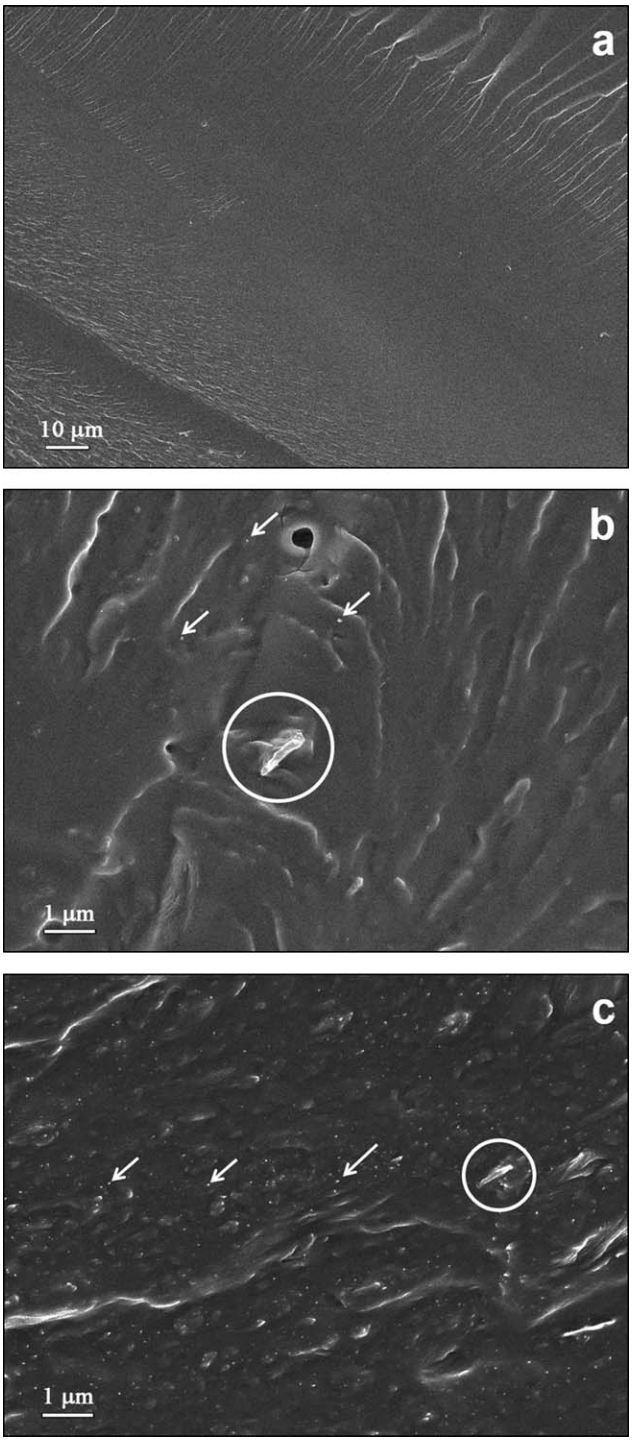

Figure 6. FESEM images of fractured surface morphologies of (a) CA/TEC, (b) D-CA/TEC/CNC15, and (c) PD-CA/TEC/CNC15 composites.

transitions, such as the glass transition (T_g) and melt temperatures. The main transitions usually observed for CA are the glass transition temperature and the β relaxation, the latter being associated to the relaxation of CA main chain glucose rings.[40,54] In this work, a T_g at 72 °C and a β relaxation peak, at approximately −20 °C, were observed for CA/TEC and composites. Based on this, it is possible to conclude that the CNC addition method does not significantly change the thermal properties of the polymer matrix. However, the addition of CNC in the CA/TEC matrix resulted in a slight widening of the glass transition associated peaks. This is an indicative of the presence of a wider range of relaxation times in the sample, which is associated to an increased number of microenvironments due to different compositions and interaction densities at the composites.[55] This peak width increase was slightly more pronounced at the PD-CA/TEC/CNC15, probably due to the better dispersion of CNC in this composite.

A tensile test specimen photograph of CA/TEC and CA/TEC/CNC composites containing 15 wt % CNC is shown in Figure S1 (Supporting Information). It is possible to observe that the CA/TEC is transparent, as plasticized CA is an amorphous thermoplastic. On the other hand, both composites are opaque, probably due to the presence of CNC aggregates and partially hydrolyzed fibers, however not visible to the naked eye. Apart from this, no black dots or yellowish color were observed in the composite specimens, which show the absence of nanocrystal and/or polymeric matrix thermal degradation.

Tensile tests were performed at room temperature and 50% relative humidity. The strength, elongation at break and Young's modulus for CA/TEC and composites, together with representative stress–strain curves, are shown in Figure 5. It can be seen that for all compositions tested, irrespective of the preparation method, the tensile strength and the elongation at break decreased with increasing CNC content [Figure 5(b,c)]. In composites prepared by direct mixture (conventional processing route), no significant changes in Young's modulus with the addition of CNC were observed. On the other hand, samples prepared by the predispersion method containing 10 and 15 wt % CNC showed a 5 and 14% Young's modulus increase, respectively [Figure 5(d)]. The increase in the elastic modulus is due to the introduction of rigid nanoparticles into the polymer matrix and can be used as evidence of the stress transfer between the CNC and the matrix. However, the improvement in elastic modulus observed in this work was low when compared to results already reported in literature, as presented in some detail in the following paragraph.

Herrera *et al.*[56] found a 267 and 50% increase in elastic modulus in composites based on plasticized poly(lactic acid) by adding 1 wt % of CNC prepared using two cooling rates. Bondeson and Oksman[35] also reported an improvement of 380 MPa at 80 °C using HCl-hydrolyzed whiskers to reinforce plasticized CA butyrate. On the other hand, by predispersing 2 wt % of CNC into a CA butyrate/TEC alcoholic solution, Hooshmand *et al.*[48] observed a decrease in composite mechanical properties. As described by the authors, changes in mechanical properties of CNC-based composites are related to the formation of CNC agglomerates. Dufresne[34] attributes the mechanical performance of CNC containing composites to CNC hydrogen bonding interactions that govern the percolation network formation.

The mechanical percolation threshold for rod-like nanoparticles in a polymeric matrix can be estimated from the following equation:

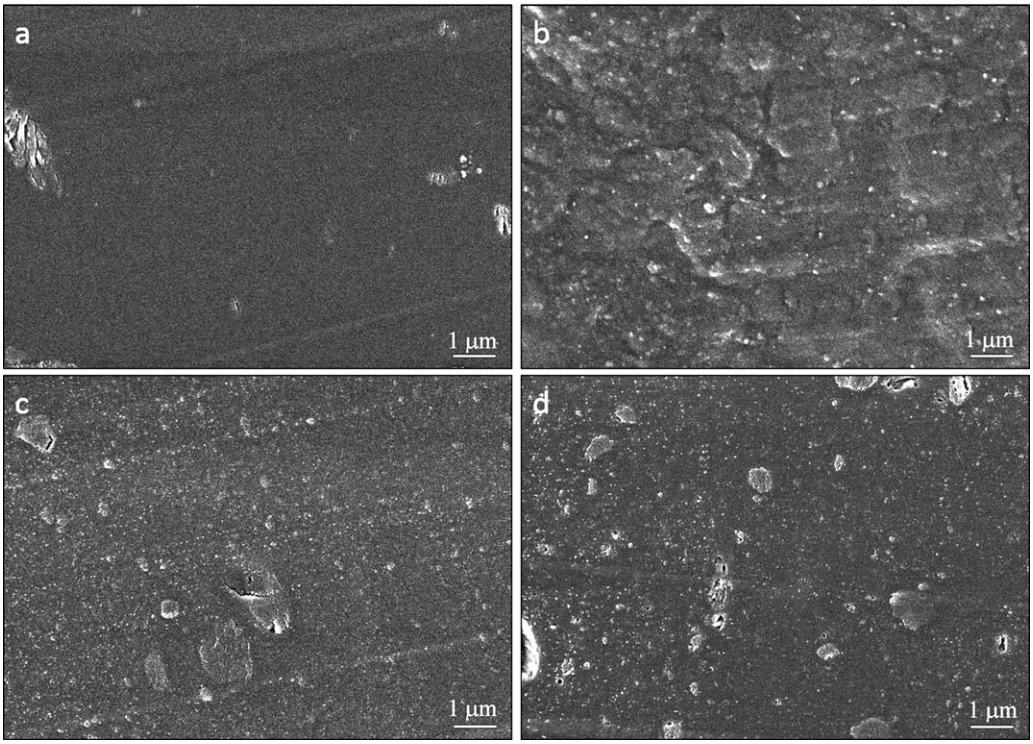

Figure 7. FESEM micrographs of cryo-ultramicrotomed surfaces of D-CA/TEC/CNC15 (a) parallel and (b) perpendicular to the injection flow and PD-CA/TEC/CNC15 (c) parallel and (d) perpendicular to the injection flow.

$$\upsilon_{Rc}=0.7/(L/d) \quad (2)$$

where L/d is the aspect ratio, assuming a cylindrical shape for the nanofiller, and υ_{Rc} is the percolation threshold.[9,29,57] Assuming the calculated L/d of 16 mentioned earlier, the corresponding percolation threshold for the CNC studied herein is 4.4 vol %, which gives approximately 5.1 wt % CNC considering the 1.3 and 1.5 g/cm^3 density values for CA and CNC, respectively.

Recent work on CNC composites has been showing that, notwithstanding the preparation method, improvements in mechanical properties are observed in loadings well above the mechanical percolation threshold. Dong *et al.*[58] reported a 17% storage modulus gain in poly(methyl methacrylate)/CNC nanocomposites, obtained by electrospining, when 17 wt % CNC was added to the polymer. On the other hand, Habibi *et al.*[59] observed that when functionalized CNC, at a range of 10% to 40 wt %, is added to a polycaprolactone matrix, continuous improvement in Young's modulus is observed. In these studies, the estimated percolation thresholds are 3.9 wt % and 3.2 wt %, respectively.

In the present work, although the CNC contents used in the composites were above the calculated percolation threshold (5.1 wt %), the effect of the CNC addition on the mechanical properties was dependent on the composite preparation method. In an attempt to evaluate CNC dispersion and distribution in composites obtained by different methods, FESEM and TEM analyses were carried out. FESEM of cryogenically fractured samples are shown in Figure 6. A smooth fractured surface is observed for the CA/TEC matrix [Figure 6(a)]. On the other hand, D-CA/TEC/CNC15 and PD-CA/TEC/CNC15 showed rough fractured surfaces where partially hydrolyzed fibers (circles), as well as white dots (arrows) are observed. The presence of white dots can be assigned to small CNC aggregates [Figure 6(b,c)]. Both CNC aggregates and partially hydrolyzed fibers showed good interfacial adhesion to the matrix. The presence of white dots is assigned to the cross-sections of the nanocrystals embedded in the polymer matrix and were also reported in literature.[29,31,60]

In this work, the composite prepared by the predispersion method showed a higher white dot density and a more uniform distribution in the polymer, as compared to that prepared by the direct mixture method. The average size of the white dots presented in the PD-CA/TEC/CNC15 sample was 21 ± 4 nm, which may correspond to aggregates formed from few nanoparticles. On the other hand, the average size of the white dots in the D-CA/TEC/CNC15 was higher (56 ± 21 nm). These differences can be related to the CNC addition method used. In conventional processing, powdered CNC (obtained from the freeze drying process) was directly mixed with the matrix, while in the predispersion method, a CNC concentrated film obtained by solvent casting was powdered, added to the polymer and processed. CNC drying step, carried out before processing (direct mixture) can lead to the formation of particle aggregates, which may not redisperse well during melt extrusion. These nanocrystal aggregates are highly organized structures stabilized by CNC contacts and formed as a consequence of the removal of water.[61]

It is important to point out that the presence of the partially hydrolyzed fibers indicates a lower CNC content than planned.

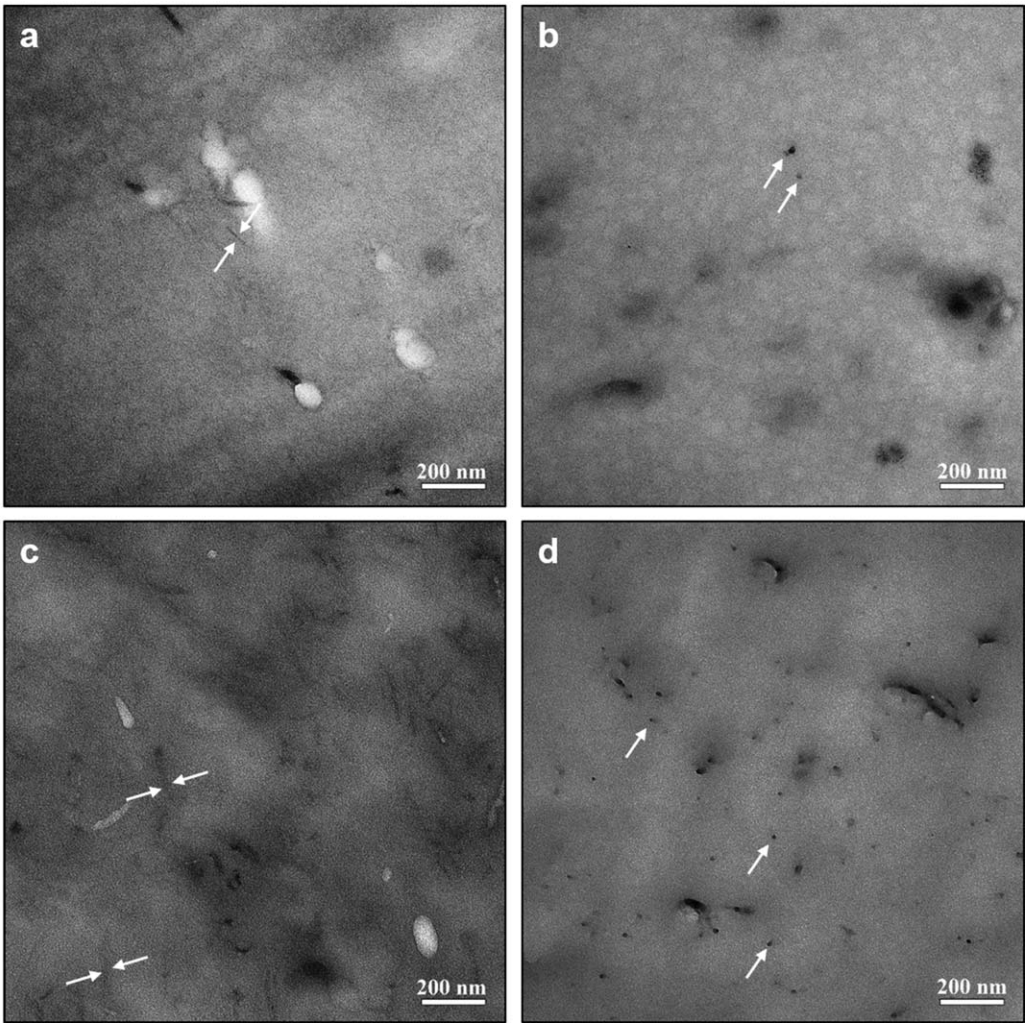

Figure 8. TEM micrographs of D-CA/TEC/CNC15 (a) parallel and (b) perpendicular to the injection flow and PD-CA/TEC/CNC15 (c) parallel and (d) perpendicular to the injection flow.

This is a result of the absence of charged groups on the CNC surface, which is characteristic of the hydrochloric acid hydrolysis. If on the one hand, this is responsible for the increased thermal stability, on the other hand, it impairs the formation of stable CNC suspensions, which are crucial for CNC isolation. Therefore, the separation of partially hydrolyzed fibers and nanocrystals is unfeasible. Based on this, it is possible to consider that the percolation threshold value could not be reached in this work, even for the highest CNC content used (15 wt %).

To avoid effects caused in microscopic observation by the fracture roughness, samples were also prepared by cryo-ultramicrotomy in two different directions: perpendicular and parallel to the injection flow. The analysis of these cross-sections shows that the use of the predispersion method [Figure 7(c,d)] resulted in an improvement of the CNC dispersion and distribution in the CA/TEC matrix, when compared to the direct mixture [Figure 7(a,b)]. Image of the D-CA/TEC/CNC15 composite perpendicular cross-section shows the presence of a larger number of white dots when compared to the same composite parallel cross-section. On the other hand, the PD-CA/TEC/CNC15 composite shows the similar distribution of white dots on both directions. Probably this difference in the nanocrystal dispersion and distribution can be the main factor contributing to the improved mechanical properties of PD-CA/TEC/CNC15 composite. Therefore, this composite preparation method may promote the percolation network formation.

Figure 8 shows the TEM images of the composite ultrathin sections. It is important to point out that TEM images of polymer composites containing CNC are quite rare in literature due to the low contrast between the CNC nanoparticles and polymeric matrices. Moreover, the similar chemical composition of CNC and CA makes CNC staining difficult. As a consequence, the interface between CNC and CA is diffuse in the TEM micrographs shown in this work. To confirm the presence of CNC in the CA matrix, a uranium mapping of PD-CA/TEC/CNC15 was performed. The electron spectroscopic image (ESI-TEM) presented in Figure S2 (Supporting Information) shows uranium-rich regions, which may be attributed to CNC.

Both D-CA/TEC/CNC15 and PD-CA/TEC/CNC15 present CNC needle-like structures (arrows) dispersed in the CA/TEC matrix,

as well as small CNC agglomerates. TEM images also show a higher content of dispersed CNC in the PD-CA/TEC/CNC15 composite [Figure 8(c,d)], compared to the D-CA/TEC/CNC15 composite [Figure 8(a,b)], which is in agreement with the FESEM observations. Apart from this, the presence of a large content of black dots in the PD-CA/TEC/CNC15 composite, obtained from the ultrathin section perpendicular to the injection flow direction [Figure 8(d)], suggests that the CNC are oriented to the injection flow. On the other hand, the TEM micrograph of the PD-CA/TEC/CNC15 composite, obtained from the ultrathin section parallel to the injection flow [Figure 8(c)], has no preferential orientation in relation to the image plane.

The results obtained in this work showed that, besides the CNC content and the need for good CNC dispersion and distribution in the polymeric matrix, the formation of the percolation network may be further considered from the particle-particle interaction viewpoint. In this regard, the CNC predispersion in the CA/TEC matrix by solvent casting can play an important role as it avoids the CNC drying step and consequently CNC aggregation. Therefore, predispersion of CNC can facilitate the percolation network formation.

In conclusion, although the mechanical properties of these composites do not present pronounced improvements, the results obtained in this work show that the CNC needle-like morphology was preserved after composite processing. Finally, the microscopic study of the composites showed that the preparation method is a key issue in CNC-based composites.

CONCLUSIONS

The hydrochloric acid hydrolysis resulted in thermally stable CNC, which allowed them to be used in the melt extrusion process. The predispersion of CNC in CA/TEC solution prior to processing has been proven to be advantageous when compared to the conventional processing route, as it allows better CNC dispersion and distribution, as proven by the FESEM and TEM micrographs. The predispersion method also promoted CNC orientation in direction to the injection flow. This is a straightforward alternative to CNC composite preparation, as it improves CNC dispersion and distribution without the need for CNC drying or functionalization. The results obtained in this work give important insights concerning the morphology of CNC-based composites, showing that to achieve the percolation threshold nanoparticle distribution is as important as their content.

ACKNOWLEDGMENTS

This research was supported by Fundação de Amparo à Pesquisa do Estado de São Paulo (FAPESP), Conselho Nacional de Desenvolvimento Científico e Tecnológico (CNPq), National Institute of Science, Technology and Innovation in Complex Functional Materials (Inomat/INCT). L. C. Battirola also thanks Coordenação de Aperfeiçoamento de Pessoal de Nível Superior (CAPES) for the scholarship. The authors confirm that this article content has no conflict of interest.

REFERENCES

1. Klemm, D.; Kramer, F.; Moritz, S.; Lindström, T.; Ankerfors, M.; Gray, D.; Dorris, A. *Angew. Chem. Int. Ed. Engl.* **2011**, *50*, 5438.
2. Favier, V.; Chanzy, H.; Cavaille, J. Y. *Macromolecules* **1995**, *28*, 6365.
3. Miao, C.; Hamad, W. Y. *Cellulose* **2013**, *20*, 2221.
4. Ranby, B. G.; Rånby, B. G.; Ranby, B. G. *Discuss. Faraday Soc.* **1951**, *11*, 158.
5. Marchessault, R.; Morehead, F.; Koch, M. J. *J. Colloid Sci.* **1961**, *16*, 327.
6. Lu, P.; Hsieh, Y.-L. *Carbohydr. Polym.* **2010**, *82*, 329.
7. Camarero Espinosa, S.; Kuhnt, T.; Foster, E. J.; Weder, C.; Espinosa, S. C.; Kuhnt, T.; Foster, E. J.; Weder, C.; Camarero Espinosa, S.; Kuhnt, T.; Foster, E. J.; Weder, C. *Biomacromolecules* **2013**, *14*, 1223.
8. Rusli, R.; Shanmuganathan, K.; Rowan, S. J.; Weder, C.; Eichhorn, S. J. *Biomacromolecules* **2011**, *12*, 1363.
9. Azizi Samir, M. A. S.; Alloin, F.; Dufresne, A. *Biomacromolecules* **2005**, *6*, 612.
10. Habibi, Y.; Lucia, L. A.; Rojas, O. J. *Chem. Rev.* **2010**, *110*, 3479.
11. Lin, N.; Huang, J.; Chang, P. R.; Feng, J.; Yu, J. *Carbohydr. Polym.* **2011**, *83*, 1834.
12. Fortunati, E.; Peltzer, M.; Armentano, I.; Torre, L.; Jiménez, A.; Kenny, J. M. *Carbohydr. Polym.* **2012**, *90*, 948.
13. Goffin, A. L.; Raquez, J.-M.; Duquesne, E.; Siqueira, G.; Habibi, Y.; Dufresne, A.; Dubois, P. *Polymer (Guildf)* **2011**, *52*, 1532.
14. Follain, N.; Belbekhouche, S.; Bras, J.; Siqueira, G.; Marais, S.; Dufresne, A. *J. Membr. Sci.* **2013**, *427*, 218.
15. Gray, D. G. *Cellulose* **2008**, *15*, 297.
16. Junior de Menezes, A.; Siqueira, G.; Curvelo, A. a S.; Dufresne, A. *Polymer (Guildf)* **2009**, *50*, 4552.
17. Petersson, L.; Mathew, A. P.; Oksman, K. *J. Appl. Polym. Sci.* **2009**, *112*, 2001.
18. Siqueira, G.; Mathew, A. P.; Oksman, K. *Compos. Sci. Technol.* **2011**, *71*, 1886.
19. Edgar, K. J.; Buchanan, C. M.; Debenham, J. S.; Rundquist, P. A.; Seiler, B. D.; Shelton, M. C.; Tindall, D. *Prog. Polym. Sci.* **2001**, *26*, 1605.
20. Romero, R. B.; Leite, C. A. P.; Gonçalves, M. D. C. *Polymer (Guildf)* **2009**, *50*, 161.
21. Nielsen, H. L.; Engberg, J.; Ejlertsen, T.; Nielsen, H. *Diagn. Microbiol. Infect. Dis.* **2013**, *76*, 549.
22. Andrade, P. F.; de Faria, A. F.; Quites, F. J.; Oliveira, S. R.; Alves, O. L.; Arruda, M. A. Z.; Gonçalves, M.; do, C. *Cellulose,* **2015**, *22*, 3895.
23. Li, G.; Wang, J.; Hou, D.; Bai, Y.; Liu, H. *J. Environ. Sci.*, **2016**, *45*, 7.
24. de Moraes, A. C. M.; Andrade, P. F.; de Faria, A. F.; Simões, M. B.; Salomão, F. C. C. S.; Barros, E. B.; Gonçalves, M. D. C.; Alves, O. L. *Carbohydr. Polym.* **2015**, *123*, 217.

25. Shinde, S. M.; Kalita, G.; Sharma, S.; Zulkifli, Z.; Papon, R.; Tanemura, M. *Surf. Coat. Technol.* **2015**, *275*, 369.
26. Milovanovic, S.; Markovic, D.; Aksentijevic, K.; Stojanovic, D. B.; Ivanovic, J.; Zizovic, I. *Carbohydr. Polym.* **2016**, *147*, 344.
27. Garg, A.; Rai, G.; Lodhi, S.; Jain, A. P.; Yadav, A. K. *Int. J. Biol. Macromol.* **2016**, *87*, 449.
28. Liakos, I. L.; D'autilia, F.; Garzoni, A.; Bonferoni, C.; Scarpellini, A.; Brunetti, V.; Carzino, R.; Bianchini, P.; Pompa, P. P.; Athanassiou, A. *Int. J. Pharm.,* **2016**, DOI: 10.1016/j.ijpharma.2016.01.060.
29. Pullawan, T.; Wilkinson, A. N.; Eichhorn, S. J. *Biomacromolecules* **2012**, *13*, 2528.
30. Yang, Z.-Y.; Wang, W.-J.; Shao, Z.-Q.; Zhu, H.-D.; Li, Y.-H.; Wang, F. J. *Cellulose* **2012**, *20*, 159.
31. Moon, R. J.; Martini, A.; Nairn, J.; Simonsen, J.; Youngblood, J. *Chem. Soc. Rev.* **2011**, *40*, 3941.
32. Bondeson, D.; Syre, P.; Niska, K. O. *J. Biobased Mater. Bioenergy* **2007**, *1*, 367.
33. Sapkota, J.; Kumar, S.; Weder, C.; Foster, E. J. *Macromol. Mater. Eng.* **2015**, *300*, 562.
34. Dufresne, A. *Can. J. Chem.* **2008**, *86*, 484.
35. Bondeson, D.; Oksman, K. *Compos. Part A: Appl. Sci. Manuf.* **2007**, *38*, 2486.
36. Correa A. C.; Teixeira, E. M.; Carmona, V. B.; Teodoro, K. B.; Ribeiro, C.; Mattoso, L. H. C.; Marconcini, J. E. *Cellulose*, **2014**, *21*, 311.
37. Pracella, M.; Haque, M. M. - U.; Puglia, D. *Polymer (Guildf)* **2014**, *55*, 3720.
38. de Oliveira Taipina, M.; Ferrarezi, M. M. F.; Yoshida, I. V. P.; Gonçalves, M. D. C. *Cellulose* **2013**, *20*, 217.
39. Araki, J.; Wada, M.; Kuga, S.; Okano, T. *Colloids Surf. A Physicochem. Eng. Aspects* **1998**, *142*, 75.
40. Gutiérrez, M. C. D.; Paoli, M.-A.; Felisberti, M. I. *Compos. Part A: Appl. Sci. Manuf.* **2012**, *43*, 1338.
41. Segal, L.; Creely, J. J.; Martin, A. E.; Conrad, C. M. *Text. Res. J.* **1959**, *29*, 786.
42. Martins, M. A.; Teixeira, E. M.; Corrêa, A. C.; Ferreira, M.; Mattoso, L. H. C. *J. Mater. Sci.* **2011**, *46*, 7858.
43. Dufresne, A. *Mater. Today* **2013**, *16*, 220.
44. Bras, J.; Viet, D.; Bruzzese, C.; Dufresne, A. *Carbohydr. Polym.* **2011**, *84*, 211.
45. Oliveira Taipina, M.; Ferrarezi, M. M. F.; Gonçalves, M. D. C. *Cellulose* **2012**, *19*, 1199.
46. Oksman, K.; Bondeson, D.; Syre P. U.S. Patent 2008/0108772 A1, May 08 **2008**.
47. Hooshmand, S.; Cho, S.-W.; Skrifvars, M.; Mathew, A.; Oksman, K. *Plast. Rubber Compos.* **2014**, *43*, 15.
48. Chatterjee, P. K.; Conrad, C. M. *J. Polym. Sci. Part A-1 Polym. Chem.* **1968**, *6*, 3217.
49. Hanna, A. A.; Basta, A. H.; El-Saied, H.; Abadir, I. F. *Polym. Degrad. Stab.* **1999**, *63*, 293.
50. Brandão, L. R.; Yoshida, I. V. P.; Felisberti, M. I.; Gonçalves, M. D. C. *Cellulose* **2013**, *20*, 2791.
51. Mariano, M.; El Kissi, N.; Dufresne, A. *Eur. Polym. J.* **2015**, *69*, 208.
52. Roman, M.; Winter, W. T. *Biomacromolecules* **2004**, *5*, 1671.
53. Wang, N.; Ding, E.; Cheng, R. *Polymer (Guildf)* **2007**, *48*, 3486.
54. Vidéki, B.; Klébert, S.; Pukánszky, B. *J. Polym. Sci. Part B Polym. Phys.* **2007**, *45*, 873.
55. Cassu, S. N.; Felisberti, M. I. *Polymer (Guildf)* **1997**, *38*, 3907.
56. Herrera, N.; Mathew, A. P.; Oksman, K. *Compos. Sci. Technol.* **2015**, *106*, 149.
57. Siqueira, G.; Bras, J.; Dufresne, A. *Polymers (Basel)* **2010**, *2*, 728.
58. Dong, H.; Strawhecker, K. E.; Snyder, J. F.; Orlicki, J. a.; Reiner, R. S.; Rudie, A. W. *Carbohydr. Polym.* **2012**, *87*, 2488.
59. Habibi, Y.; Goffin, A.-L.; Schiltz, N.; Duquesne, E.; Dubois, P.; Dufresne, A. *J. Mater. Chem.* **2008**, *18*, 5002.
60. Ben Azouz, K.; Ramires, E. C.; Van den Fonteyne, W.; El Kissi, N.; Dufresne, A. *ACS Macro Lett.* **2012**, *1*, 236.
61. Peng, Y.; Gardner, D. J.; Han, Y. *Cellulose* **2012**, *19*, 91.